Article

Not peer-reviewed version

# COF-SiO2@Fe3O4 Core-Shell Composite for Magnetic Solid-Phase Extraction of Pyrethroid Pesticides in Vegetables

Ling Yu *, Aiqing Xia , Yongchao Hao , Weitao Li , Cuijuan Xing *, Zan Shang , Yiwei Zhang

Posted Date: 19 February 2024

doi: 10.20944/preprints202402.0937.v1

Keywords: covalent organic framework; magnetic solid-phase extraction; gas chromatography-mass spectrometry; pyrethroids pesticides

*Article*

# COF-$SiO_2$@$Fe_3O_4$ Core-Shell Composite for Magnetic Solid-Phase Extraction of Pyrethroid Pesticides in Vegetables

**Ling Yu *, Aiqing Xia, Yongchao Hao, Weitao Li, Cuijuan Xing *, Zan Shang and Yiwei Zhang**

College of Chemistry and Chemical Engineering, Xingtai University, Xingtai 054001, Hebei, PR China; xiaaiqing59420@sina.com (A.X.); haoyongchao2015@163.com (Y.H.); liweitao2021xtxy@163.com (W.L.); s15530181703@163.com (Z.S.); zyw17659928836@163.com (Y.Z.)

* Correspondence: 200820347@xttc.edu.cn (L.Y.); cuijuanxing@163.com (C.X.)

**Abstract:** Pyrethroid pesticides (PYRs) as the third most widely used pesticides, following organophosphorus and carbamate pesticides, which are of significant importance in the analysis and detection of vegetables. However, the current pretreatment technology for PYRs confronts challenges of difficult separation and low enrichment efficiency, resulting in a cumbersome and time-consuming pretreatment process with poor selectivity. Here, a simple and efficient magnetic solid-phase extraction (MSPE) strategy was developed to simultaneously purify and enrich five PYRs in vegetables, with the magnetic covalent organic framework nanomaterial COF-$SiO_2$@$Fe_3O_4$ as an adsorbent. The COF-$SiO_2$@$Fe_3O_4$ was prepared by a simple solvothermal conditions method, using $Fe_3O_4$ as magnetic core, benzidine and 3,3,5,5-tetraaldehyde biphenyl as two building units. COF-$SiO_2$@$Fe_3O_4$ could effectively capture the targeted PYRs by virtue of its abundant π-electron system and hydroxyl groups. The impact of various experimental parameters on extraction efficiency was investigated to optimize the MSPE conditions, including adsorbent amount, extraction time, elution solvent type and elution time. Subsequently, method validation was conducted under the optimal conditions in conjunction with gas chromatography-mass spectrometry (GC-MS). Within the range of 5.00–100 μg·kg$^{-1}$ (1.00–100 μg·kg$^{-1}$ for bifenthrin and 2.5–100 μg·kg$^{-1}$ for fenpropathrin), the five PYRs exhibited a strong linear relationship, with determination coefficients ranging from 0.9990 to 0.9997. The limits of detection (LODs) were 0.3–1.5 μg·kg$^{-1}$, and the limits of quantification (LOQs) were 0.9–4.5 μg·kg$^{-1}$. The recoveries were 80.2–116.7% with relative standard deviations (RSDs) below 7.0%. Finally, COF-$SiO_2$@$Fe_3O_4$, $NH_2$-$SiO_2$@$Fe_3O_4$ and $Fe_3O_4$ were compared as MSPE adsorbents for PYRs. The results indicated that COF-$SiO_2$@$Fe_3O_4$ was an efficient and rapid selective adsorbent for PYRs. This method holds promising prospects for the determination of PYRs in real samples.

**Keywords:** covalent organic framework; magnetic solid-phase extraction; gas chromatography-mass spectrometry; pyrethroids pesticides

## 1. Introduction

Pyrethroids pesticides (PYRs) were a class of synthetic insecticides in the 1970s and possessed low cost, wide insecticidal, low toxicity, low residue and environmental friendliness. They played an important role in pest control and were widely used in the production of vegetables, fruits and other agricultural products. 1. However, growing evidence indicates that PYRs may be endocrine disruptors, which can impair the endocrine function of animals and have estrogenic effects on the environment 2. Toxic substances can kill embryos prior to and after implantation, or malformations of various organs 3. Long-term exposure to pyrethroids and their metabolites may lead to endocrine-disrupting effects and sublethal toxicity. With the increasing awareness of food safety, some organizations have established the maximum residue limits (MRLs) of PYRs in fruits and vegetables, such as 0.01–0.5 mg·kg$^{-1}$ in the European Union 4 and 0.01–10 mg·kg$^{-1}$ in China (GB 2763-2021). Therefore, it is of great significance to establish a simple, rapid and accurate detection method for PYRs.

 doi:10.20944/preprints202402.0937.v1



The matrix of vegetable samples contains large amounts of pigments, cellulose and minerals, which could dramatically impede the detection of trace PYRs in food. Therefore, efficient enrichment and purification of multiple PYRs in vegetable samples is crucial before instrumental analysis. Recently, the sample preparation method for pesticide residue analysis in vegetable mainly involves liquid-liquid extraction (LLE) 5, QuEChERS methods 6,7 and solid-phase extraction (SPE) 8. SPE has obvious advantages in enrichment of analytes, purification of matrix, and low organic solvent consumption 9. Compared to LLE and QuEChERS, SPE is more suitable for sample pretreatment of trace components in complex matrix samples. However, the SPE procedure is usually expensive, time consuming and tedious.

Magnetic solid-phase extraction (MSPE) has the advantages of easy separation, convenient operation and time-saving qualities1011. In the MSPE process, the magnetic sorbents are directly dispersed in the sample solution for rapid and efficient extraction of analytes, and then quickly separated by an external magnetic field. MSPE effectively compensates for the shortcomings of SPE. At present, MSPE is widely used in the field of environmental governance 1213, biotechnology 1415, medicine 16 and food 17,18. MSPE technology mainly relies on magnetic $Fe_3O_4$ nanoparticles and their surface adsorbent, which significantly affects the selectivity and efficiency of a MSPE approach. Recently, novel porous materials such as molecularly imprinted polymers (MIPs) 1920, porous carbon 2122, microporous organic networks (MONs) 2324 and metal organic frameworks (MOFs) 25,26 have been employed as adsorbents for separation and enrichment. However, they still have drawbacks such as low adsorption capacity, poor selectivity and weak temperature tolerance, which limit their applications to some extent. Therefore, it is urgently needed to explore the adsorbents with excellent extraction performanc to solve these problems.

Covalent organic framework (COF) is a new type of porous polymer material, which can be constructed with organic building units by covalent bonds of elements (C, O, N, H, etc.) 26. The structure and surface properties are mainly dependent on covalently linked topological schemes and organic monomers. It has excellent characteristics such as adjustable pore size and high chemical stability, making it have superior application potential for a variety of applications, such as catalysis 2828, sensing 30, optoelectronic devices **Error! Reference source not found.** and separation 3133. In this paper, the target analyte PYRs contains benzene rings and heteroatoms. Benzidine and 3,3,5,5-tetraaldehyde biphenyl was selected as ligands to synthesize the COF material with π- electron system and enriched hydroxyl groups in the structure. And the strong π-π stacking and hydrophobic interactions of the COF and PYRs leads to better adsorption properties. However, the inconvenient separation of COFs from solution due to COFs low density is a challenge and limits their application in the field of separation and enrichment. Fortunately, the combination of COFs and $Fe_3O_4$ provides a pathway to solve the above problem and reduce large mass loss of COFs.

During this study, a new core-shell material, COF-$SiO_2$@$Fe_3O_4$, was successfully synthesized under solvothermal conditions. Using it as an extractant, combined with GC-MS, a sample pretreatment method for MSPE of trace amounts of PYRs in vegetables was established. The synthesized COF-$SiO_2$@$Fe_3O_4$ has the advantages of good thermal stability, fast separation ability, and good selectivity for PYRs. At the same time, COF-$SiO_2$@$Fe_3O_4$ can be collected quickly through magnets, which is environmentally friendly. The developed MSPE-GC-MS method utilizing COF-$SiO_2$@$Fe_3O_4$ composites was applied for the enrichment and determination of PYRs in vegetables. A schematic diagram of the synthesis of COF-$SiO_2$@$Fe_3O_4$ and determination of PYRs by MSPE is shown in Scheme 1.

 doi:10.20944/preprints202402.0937.v1



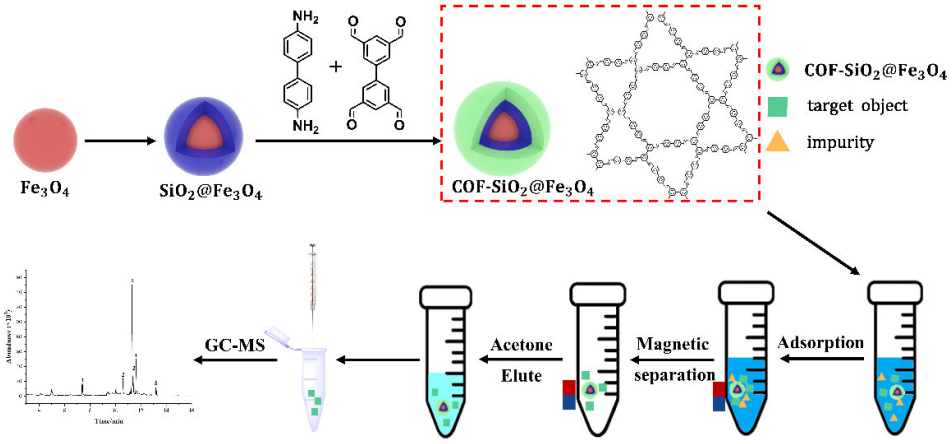


**Scheme 1.** Synthesis of COF-$SiO_2$@$Fe_3O_4$ and determination of PYRs by MSPE.

## 2. Results and Discussion

### *2.1. Characterization of COF-$SiO_2$@$Fe_3O_4$*

The surface morphology of the prepared materials was characterized by SEM and TEM. The SEM images of $Fe_3O_4$, COF-$SiO_2$@$Fe_3O_4$ and the TEM images of COF-$SiO_2$@$Fe_3O_4$ were shown in Figure 1. It can be seen that the $Fe_3O_4$ materials presents a spherical structure with rough surface (Figure 1a). After the modification of a COF shell, a relatively smooth surface was observed in the SEM image of COF-$SiO_2$@$Fe_3O_4$ (Figure 1b). Through TEM combined with mapping analysis, COF-$SiO_2$@$Fe_3O_4$ contains five elements of Fe, C, O, Si and N, which proves the successful synthesis of COF-$SiO_2$@$Fe_3O_4$. Among them, the contents of Fe, C and O elements were mostly 25%, 37% and 35%, respectively. The C element was mainly derived from the synthesis of covalent organic frameworks, and the N element was mainly derived from the ligand benzidine. The core-shell structure of COF-$SiO_2$@$Fe_3O_4$ can be clearly seen by mapping.

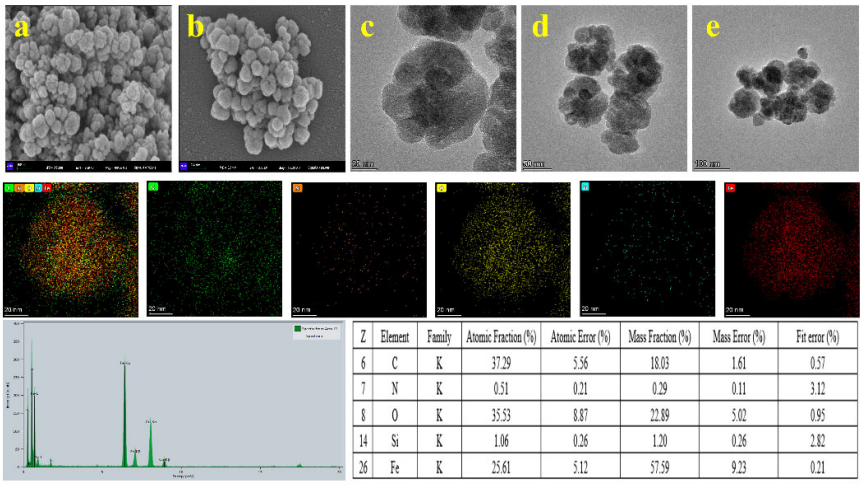


| Z | Element | Family | Atomic Fraction (%) | Atomic Error (%) | Mass Fraction (%) | Mass Error (%) | Fit error (%) |
|---|---|---|---|---|---|---|---|
| 6 | C | K | 37.29 | 5.56 | 18.03 | 1.61 | 0.57 |
| 7 | N | K | 0.51 | 0.21 | 0.29 | 0.11 | 3.12 |
| 8 | O | K | 35.53 | 8.87 | 22.89 | 5.02 | 0.95 |
| 14 | Si | K | 1.06 | 0.26 | 1.20 | 0.26 | 2.82 |
| 26 | Fe | K | 25.61 | 5.12 | 57.59 | 9.23 | 0.21 |

**Figure 1.** SEM images of $Fe_3O_4$ (a), COF-$SiO_2$@$Fe_3O_4$ (b), TEM images of COF-$SiO_2$@$Fe_3O_4$ (c), (d), (e) and mapping images.

The XRD patterns of $Fe_3O_4$, $SiO_2$@$Fe_3O_4$, $NH_2$-$SiO_2$@$Fe_3O_4$ and COF-$SiO_2$@$Fe_3O_4$ materials were shown in Figure 2. In Figure 2a, characteristic diffraction peaks could be observed at 2θ=30.1° (200), 35. 5° (311), 43.5° (400), 53.7° (422), 57.2° (511) and 62.5° (440), which were all attributed to the magnetic center body, indicating that the synthesized material has a good crystal structure [34. In the XRD pattern of $SiO_2$@$Fe_3O_4$, there were no other diffraction peaks emerged, indicating that the coated

 doi:10.20944/preprints202402.0937.v1



$SiO_2$ shell was amorphous. For COF-$SiO_2$@$Fe_3O_4$, the newly appeared peaks located at 2θ=16.3° was speculated to be related to the encapsulation of COF. Compared with $Fe_3O_4$, the characteristic peaks of $SiO_2$@$Fe_3O_4$, $NH_2$-$SiO_2$@$Fe_3O_4$ and COF-$SiO_2$@$Fe_3O_4$ were not significantly different, indicating that the gradual reaction of $Fe_3O_4$ to COF-$SiO_2$@$Fe_3O_4$ does not cause changes in the crystal phase.

The infrared spectra of $Fe_3O_4$, $SiO_2$@$Fe_3O_4$, $NH_2$-$SiO_2$@$Fe_3O_4$ and COF-$SiO_2$@$Fe_3O_4$ (4000–500 $cm^{-1}$) were shown in Figure 2b. The characteristic peak at 3440 $cm^{-1}$ was the stretching vibration peak of -OH group. The typical band at 577 $cm^{-1}$ was assigned to the Fe-O-Fe vibration, which was the evidence for the existence of $Fe_3O_4$. The characteristic band at 1640 $cm^{-1}$ indicated the presence of carboxyl groups (curve a) [35. The peak at 1080 $cm^{-1}$ was the tensile vibration of the Si-O group (curve b), indicating that $SiO_2$ had been successfully loaded onto the surface of the particles. After the amination modification of $Fe_3O_4$@$SiO_2$, a new peak appears at 1560 $cm^{-1}$ (curve c), which was -$NH_2$ on the surface of $SiO_2$ nanoparticles. The peak was disappeared after the formation of COF-$SiO_2$@$Fe_3O_4$, but new peaks appeared at 1250 $cm^{-1}$ and 1480 $cm^{-1}$, corresponding to C=N and aromatic C=C groups, respectively (curve d), indicating that COF was successfully attached to the surface of magnetic nanoparticles. The above results showed that COF-$SiO_2$@$Fe_3O_4$ was successfully synthesized by covalent bonding between monomers.

The saturation magnetization values of the $Fe_3O_4$, $SiO_2$@$Fe_3O_4$, $NH_2$-$SiO_2$@$Fe_3O_4$ and the COF-$SiO_2$@$Fe_3O_4$ nanocomposites were measured to be 71.85, 68.67, 67.97 and 59.59 emu·$g^{-1}$, respectively. The hysteresis curves of all magnetic nanoparticles were S-type, which indicated their superparamagnetic characteristics (Figure 2c). Among them, the magnetization of COF-$SiO_2$@$Fe_3O_4$ was the lowest, which was 12.26 emu·$g^{-1}$ lower than that of $Fe_3O_4$. This was due to the decrease of magnetism caused by the COF wrapped on $Fe_3O_4$. Such high saturation magnetism of the COF-$SiO_2$@$Fe_3O_4$ nanocomposites was sufficient to achieve the demand for magnetic separation. As displayed in the inset of Figure 2C, the COF-$SiO_2$@$Fe_3O_4$ nanocomposites homogeneously dispersed in aqueous solution could be rapidly gathered in 0.5 min together with the assistance of an external magnet, and thus the solution became clear and transparent immediately.

The mass ratios of different components and the thermal stability of $NH_2$-$SiO_2$@$Fe_3O_4$ and COF-$SiO_2$@$Fe_3O_4$ nanocomposites were examined by TGA. As presented in Figure 2d. The temperature detection range was between 30°C and 800°C, and the heating rate was 10°C·$min^{-1}$. The $NH_2$-$SiO_2$@$Fe_3O_4$ and COF-$SiO_2$@$Fe_3O_4$ showed 8.19 wt% and 17.05 wt% loss in the temperature range of 30°C–800°C, respectively. The $NH_2$-$SiO_2$@$Fe_3O_4$ showed 1.26 wt% loss below 140 °C, which was attributed to the weight loss of the volatilization of water adsorbed on the COF-$SiO_2$@$Fe_3O_4$ structure [36. The mass loss between 140°C and 640°C is 6.26 wt%, which is the loss of amino groups. The COF-$SiO_2$@$Fe_3O_4$ showed 0.92 wt% loss below 200°C, which was attributed to the weight loss of the absorbed water. The mass loss between 200 °C and 800 °C was 14.83 wt%, mainly due to the loss of surface COF shell.

 doi:10.20944/preprints202402.0937.v1



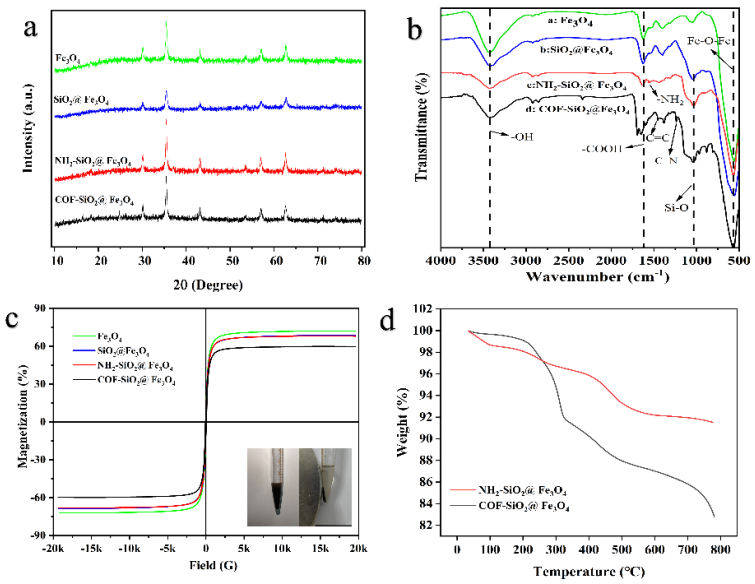


**Figure 2.** (a) XRD: $Fe_3O_4$, $SiO_2$@$Fe_3O_4$, $NH_2$-$SiO_2$@$Fe_3O_4$, COF-$SiO_2$@$Fe_3O_4$, (b) FI-IR: a-$Fe_3O_4$, b-$SiO_2$@$Fe_3O_4$ c-$NH_2$-$SiO_2$@$Fe_3O_4$, d-COF-$SiO_2$@$Fe_3O_4$, (c) VSM: $Fe_3O_4$, $SiO_2$@$Fe_3O_4$, $NH_2$-$SiO_2$@$Fe_3O_4$, COF-$SiO_2$@$Fe_3O_4$, (d) TGA: $NH_2$-$SiO_2$@$Fe_3O_4$, COF-$SiO_2$@$Fe_3O_4$.

*2.2. Optimization of MSPE Parameters*

Effect of Adsorbent Amount

The adsorbent amount plays an important role in the MSPE process and was optimized with the COF-$SiO_2$@$Fe_3O_4$ adsorbents ranging from 5 to 25 mg. As shown in Figure 3a, the recoveries presented a significantly enhanced when the employed adsorbent amount was changed from 5 to 10 mg, and then the increase of adsorbent amount did not enhance the extraction efficiency of the five PYRs. Therefore, in order to improve the recoveries and save the amount of adsorbent, 10 mg of COF-$SiO_2$@$Fe_3O_4$ was optimal and used as the adsorbent in subsequent experiments.

Effect of Extraction Time

The extraction time usually has some effects on the extraction efficiency of MSPE. Insufficient extraction time will lead to inadequate adsorption, and while too long extraction time was not necessary and might bring about some losses. The effect of extraction time was explored under vigorous oscillation for 5, 10, 15, 20 min, and the results were shown in Figure 3b. When the extraction time was 10 min, the recoveries were the highest, indicating that the adsorption between the adsorbent and the target component reached dynamic equilibrium. The recoveries decreased slightly when the extraction time was prolonged. This was because the COF-$SiO_2$@$Fe_3O_4$ adsorption site was completely occupied, and the saturated adsorption capacity was obtained at 10 min. After that, a small amount of analyte broke away from the adsorbent surface and re-entered the sample solution because the adsorption was not firm. Therefore, 10 min was sufficient for the extraction process and chosen as the preferred extraction time.

Effect of Elution Solvent

The selection of suitable elution solvent is very important for the efficient desorption of target analytes from the extracted adsorbents. Here, acetonitrile, methanol and acetone were respectively used as the elution solvent to evaluate the elution performances. As shown in Figure 3c, acetone was employed as the elution solvent significantly improve the desorption efficiency of the target compounds. The recoveries of allethrin were low, when methanol was used as eluent solvent. The

 doi:10.20944/preprints202402.0937.v1



recoveries of five PYRs were generally low when acetonitrile was used as eluent solvent. Therefore, acetone was selected as the best eluent solvent in the subsequent experiments.

Effect of Elution Time

The effect of elution time was explored under ultrasound of 1, 3, 5, 7 min, and the results were shown in Figure 3d. When increasing from 1 min to 3 min, the recoveries increased by 80–109%. When the elution time increased from 3 to 5 min, the recoveries of PYRs remained basically unchanged, because the adsorption and desorption equilibrium was reached at 3 min. When the ultrasonic time increased from 5 to 7 min, the recoveries of PYRs increased slightly. This may be due to ultrasonic heat release, which makes the organic solvent volatilize, resulting in an increase in PYRs concentration in acetone. Therefore, 3 min was selected as the best elution time.

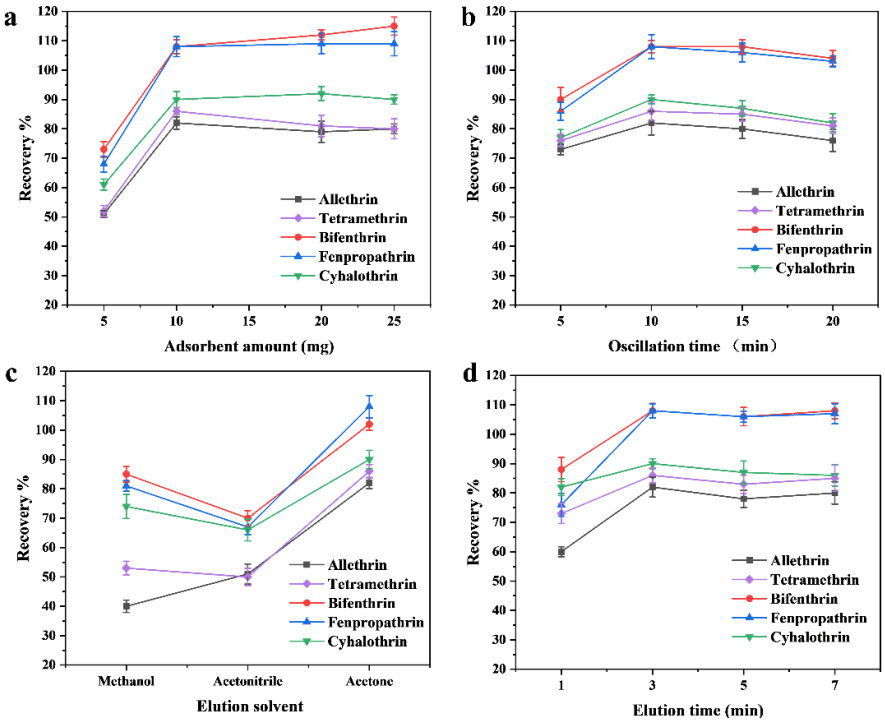


**Figure 3.** Optimization of adsorbent amount (a), extraction time (b), elution solvent (c) and elution time (d).

*2.3. Adsorption Mechanism of PYRs*

The adsorption behavior of adsorbents to target analytes is affected by their structures. According to the structures of COF-$SiO_2$@$Fe_3O_4$ and PYRs, it can be inferred that there are two main factors affecting the adsorption process. On the one hand, the surface functional groups (–$NH_2$, –OH, C=N) of COF-$SiO_2$@$Fe_3O_4$ and PYRs have strong hydrogen bond interactions [37. On the other hand, from the structural formula of PYRs, PYRs possess abundant benzene rings and have strong π-π stacking interactions with the synthesized COF-$SiO_2$@$Fe_3O_4$ with π-π conjugation [38.

*2.4. Method Validation*

The quantitative analysis of the five PYRs were further evaluated by COF-$SiO_2$@$Fe_3O_4$ based MSPE coupled with GC-MS. With the optimized conditions, method validations were also studied here, including linearity, limits of detection (LODs, S/N=3), limits of quantification (LOQs, S/N = 10), enrichment factors (EFs) and reproducibility. The results were summarized in Table 1. The good linearity of the developed method was obtained with correlation coefficients (r) higher than 0.9990 in the range of 5–100 μg·$kg^{-1}$ (1.00–100 μg·$kg^{-1}$ for bifenthrin and 2.5–100 μg·$kg^{-1}$ for fenpropathrin,

 doi:10.20944/preprints202402.0937.v1



respectively). The LODs for the five PYRs were calculated to be 0.3–1.5 μg·kg$^{-1}$. Their corresponding LOQs were found to be 0.9–4.5 μg·kg$^{-1}$. The EFs of PYRs, defined as the ratio of the concentration of the analytes in the extract to that in the original sample, were ranged from 4.4–12.4. The inter-day RSDs were obtained by extracting standard solution five times within a day, and the intra-day RSDs were determined by extracting standard solution that had been independently prepared for contiguous six days. The inter- and intra-day RSDs were in the range of 1.9–6.2% and 2.3–7.0%, respectively, indicating the acceptable reproducibility. In addition, the reproducibility of the COF-$SiO_2$@$Fe_3O_4$ nanocomposites was assessed by the batch-to-batch RSDs. The result showed that the batch-to-batch RSDs were less than 4.2%, implying the good synthetic reproducibility of the COF-$SiO_2$@$Fe_3O_4$.

**Table 1.** Linear ranges, regression equations, LODs, and LOQs of five PYRs.

| Analytes | Regression equation | Linear ranges /(μg·L$^{-1}$) | r | LODs /(μg·kg$^{-1}$) | LOQs /(μg·kg$^{-1}$) | EF | RSD(%) Inter-day (n=5) Intra-day (n=6) | | | | | | Batch to batch (n=3) |
|---|---|---|---|---|---|---|---|---|---|---|---|---|---|
| | | | | | | | 5 | 10 | 20 | 5 | 10 | 20 | |
| Allethrin | y = 616.9x - 1255.5 | 5-100 | 0.9991 | 1.5 | 4.5 | 4.4 | 3.1 | 2.5 | 2.1 | 3.4 | 2.8 | 2.7 | 4.2 |
| Tetramethrin | y = 780.02x+754.75 | 5-100 | 0.9997 | 1.5 | 4.5 | 5.0 | 5.3 | 2.3 | 2.2 | 6.5 | 3.2 | 3.6 | 3.3 |
| Bifenthrin | y=4775.3x-3182.1 | 1-100 | 0.9990 | 0.3 | 0.9 | 12.4 | 2.1 | 6.2 | 4.8 | 2.3 | 2.3 | 4.1 | 2.5 |
| Fenpropathrin | y=1077.2x + 195.48 | 2.5-100 | 0.9991 | 1.0 | 3.0 | 10.7 | 2.6 | 3.7 | 2.4 | 3.1 | 3.0 | 2.9 | 2.6 |
| Cyhalothrin | y =451.16x-561.9 | 5-100 | 0.9995 | 1.5 | 4.5 | 11.0 | 2.2 | 2.6 | 1.9 | 2.7 | 2.6 | 7.0 | 3.0 |

*2.5. Real Sample Analysis*

In order to evaluate the reliability and feasibility of the developed method in practical application, three vegetables cucumber, cabbage and lettuce were collected for the extraction and determination of PYRs. Each sample was subjected to five repeated analyses. The results showed that any of the PYRs were not detected in the vegetables. In order to further verify the method developed in the actual sample, the recoveries were analyzed by analyzing vegetable samples mixed with different concentrations of PYRs. Therefore, the three vegetables were spiked with PYRs standards at three concentrations of 5, 10, 20 μg·kg$^{-1}$ for low, medium and high level, and the extraction procedure was conducted, with RSDs (n=3) and average recoveries given in Table 2. The recoveries of five PYRs were 80.2–116.5% with RSDs of 2.3–6.7% for cucumber, 81.7–114.7% with RSDs of 2.1–6.8% for cabbage and 81.6–116.7% with RSDs of 2.4–7.0% for lettuce. The results indicated that the proposed MPSE-GC-MS method could be used for the enrichment and determination of PYRs in complex samples.

**Table 2.** Detection results of PYRs in three samples and the spiked recoveries.

| Analytes | Spiked level / (μg·kg$^{-1}$) | cucumber Recovery (%, RSD%) | Chinese cabbage Recovery (%, RSD%) | Lettuce Recovery (%, RSD%) |
|---|---|---|---|---|
| Allethrin | 5 | 80.2 (3.5) | 81.7 (3.1) | 85.3 (7.0) |
| | 10 | 90.1 (2.9) | 91.3 (3.9) | 87.3 (5.8) |
| | 20 | 96.4 (3.4) | 102.4 (4.1) | 103.5 (6.1) |
| Tetramethrin | 10 | 116.5 (6.1) | 89.1 (5.3) | 116.1 (4.5) |
| | 20 | 97.2 (4.6) | 107.6 (4.9) | 110.2 (5.7) |
| | 50 | 111.0 (6.1) | 114.7 (5.7) | 109.6 (4.8) |
| Bifenthrin | 10 | 89.2 (5.4) | 92.9 (2.1) | 97.3 (3.6) |

 doi:10.20944/preprints202402.0937.v1



| | | | | |
|---|---|---|---|---|
| | 20 | 96.6 (2.3) | 95.3 (3.2) | 94.2 (2.4) |
| | 50 | 97.4 (3.9) | 102.7 (4.2) | 93.7 (3.4) |
| | 10 | 112.5 (6.7) | 107.5 (3.7) | 116.7 (5.7) |
| Fenpropathrin | 20 | 93.1 (5.8) | 106.9 (5.6) | 109.8 (3.2) |
| | 50 | 107.8 (3.6) | 105.2 (6.5) | 107.1 (5.1) |
| | 10 | 97.3 (2.9) | 87.4 (6.8) | 81.6 (6.5) |
| Cyhalothrin | 20 | 89.9 (4.7) | 108.5 (6.5) | 89.3 (5.6) |
| | 50 | 90.1 (5.1) | 92.3 (5.3) | 93.4 (5.4) |

*2.6. Comparison of COF-$SiO_2$@$Fe_3O_4$, $NH_2$-$SiO_2$@$Fe_3O_4$ and $Fe_3O_4$ as MSPE Adsorbents*

$Fe_3O_4$ (10 mg), $NH_2$-$SiO_2$@$Fe_3O_4$ (10 mg), COF-$SiO_2$@$Fe_3O_4$ (10 mg) were used as adsorbents for MSPE of blank Chinese cabbage extract (50 μg·kg$^{-1}$) with standard addition of PYRs, and GC-MS detection was performed. The results were shown in Figure 4. The enrichment effects of $NH_2$-$SiO_2$@$Fe_3O_4$ and COF-$SiO_2$@$Fe_3O_4$ on PYRs were better than that of $Fe_3O_4$. Using COF-$SiO_2$@$Fe_3O_4$ as the adsorbent of MSPE, the impurity peaks of the chromatographic curve are less, especially the impurities that interfere with the target allethrin are eliminated, and the accuracy of the method is improved. From the analysis of structural differences, it can be seen that COF-$SiO_2$@$Fe_3O_4$ is a COF material with benzene ring and imine group wrapped outside the magnetic core, which can produce a strong π-π stacking effect with PYRs, thus having good selectivity for PYRs.

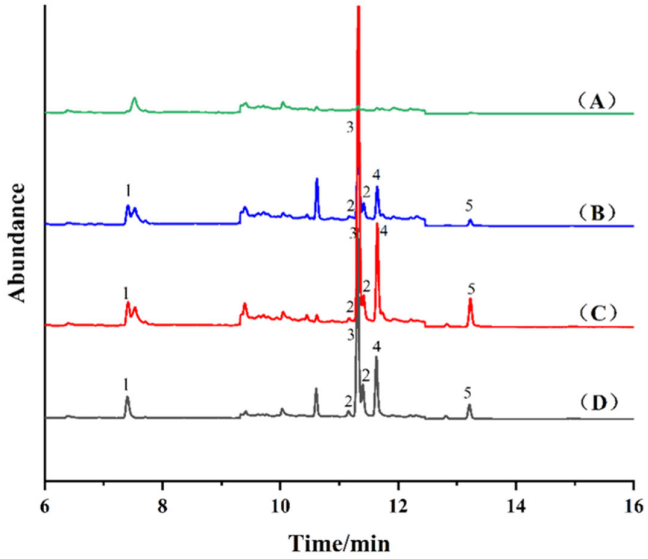


**Figure 4.** 1-Allethrin 2-Tetramethrin 3-Bifenthrin 4- Fenpropathrin 5- Cyhalothrin. Total ion fow chromatography of blank cabbage sample (A), spiked cabbage sample (50 μg·kg$^{-1}$) after purifcation by $Fe_3O_4$ (B), $NH_2$-$SiO_2$@$Fe_3O_4$ (C), COF-$SiO_2$@$Fe_3O_4$ (D), respectively.

## 3. Experimental

*3.1. Materials and Chemicals*

Benzidine (95%) and 3,3,5,5-tetraaldehyde biphenyl (97%) were purchased from Shanghai Aladdin Biochemical Technology Co., Ltd. (Shanghai, China). Allethrin, tetramethrin, bifenthrin, fenpropathrin, cyhalothrin were obtained from Beijing Putian Tongchuang Biological Technology Co., Ltd. (Beijing,China). $FeCl_3.6H_2O$ and dimethyl sulfoxide (DMSO) were purchased from Tianjin Kemiou Chemical Reagent Co., Ltd. (Tianjin, China). Anhydrous sodium acetate, ethylene glycol, anhydrous ethanol, tetrahydrofuran (THF), toluene, Tetraethoxysilane (TEOS), 3-aminopropyltriethoxysilane (APTES) and dimethyl silicone oil were purchased from Tianjin Damao Chemical Reagent Factory (Tianjin, China). Chromatographic grade acetonitrile was obtained from

 doi:10.20944/preprints202402.0937.v1



Shanghai Aladdin Biochemical Technology Co., Ltd. (Shanghai, China). Glacial acetic acid was purchased from Tianjin Fuchen Chemical Reagent Factory (Tianjin, China). Ammonia water was purchased from Yantai Far East Fine Chemical Co., Ltd. (Yantai, China).

### *3.2. Equipment*

GC/MS-QP 2010 Ultra (Shimadzu Corporation, Japan), SC-3612 centrifuge (Anhui Zhongke Zhongjia Scientific Instrument Co., LTD, China), SN-QX-20D Ultrasonic cleaning machine (Shanghai Shangdun Instrument Equipment Co., LTD, China), 2K-82B vacuum drying oven (Shanghai Instrument Experimental Factory, China), DHG-9023A blast drying oven (Shanghai Yiheng Scientific Instrument Co., LTD, China), SHB-III circulating water multi-purpose vacuum pump (Zhengzhou Great Wall Technology & Trade Co., LTD., China), RE-52AA rotary evaporator (Shanghai Yarong biochemical instrument factory, China), YTGT-12 dry nitrogen blowing instrument (Shanghai Night extension Technology Co., LTD, China), Milli-Q Ultrapure water apparatus (Millipore Corporation, USA).

Scanning electron microscopy (SEM) images were obtained with a scanning electron microscope (GeminiSEM 300, ZEISS, Germany). Transmission electron microscopy (TEM) images were recorded by a Transmission Electron Microscope (F200x, FEI Talos, USA). X-ray diffraction (XRD) data were achieved by X-ray Difraction (3kw, Rigaku, Japan). Fourier-transform infrared spectroscopy (FT-IR) was taken on Nicolet iS20 spectrometer (Thermo Fisher, USA). The magnetization curves were measured by a vibrating sample magnetometer (VSM) (7404 LakeShore, USA). Thermogravimetric analysis (TGA) was performed using a thermogravimetric analyzer (TGA/DSC 3+, Mettler Toledo, Switzerland).

### *3.3. Preparation of Standard Solution*

The stock standard solutions of five PYRs were individually prepared at the concentration of 5 $\mu g \cdot mL^{-1}$ in acetone, and stored at 4°C before use. The working standard solutions were obtained freshly before use by diluting the stock solution to the desired concentration (0.02, 0.04, 0.06, 0.08, 0.1, 0.2, 0.4 $\mu g \cdot mL^{-1}$).

### *3.4. Preparation of Magnetic Materials*

#### Synthesis of $Fe_3O_4$ magnetic nanoparticles

Monodisperse $Fe_3O_4$ magnetic nanoparticles (MNPs) were synthesized by solvothermal method [39]. Briefly, $FeCl_3 \cdot 6H_2O$ (1.352 g) and anhydrous sodium acetate (3.6 g) were dissolved in ethylene glycol (40 mL). The obtained homogeneous yellow solution was transferred to autoclave, and then heated to 200 °C for 8 h. After reaction, the product was collected by magnet and washed with ultrapure water and ethanol for several times and then dried at 60 °C in a vacuum drying oven.

#### Synthesis of $SiO_2$@$Fe_3O_4$ Magnetic Nanospheres

$Fe_3O_4$ (1 g) was dispersed in a mixture of ethanol (120 mL), ultrapure water (30 mL) and concentrated ammonia (2.4 mL). After ultrasonic dispersion for 5 min, TEOS (0.5 mL) was added and stirred for 12 h at room temperature. By hydrolysis of TEOS in an alkaline environment, the surface of $Fe_3O_4$ was coated with a silica layer containing -OH. The obtained brown precipitates were collected by magnetic separation and washed with a ultrapure water and ethanol for three times. Finally, the resultant $SiO_2$@$Fe_3O_4$ nanocomposites were dried in vacuum at 60 °C.

#### Synthesis of $NH_2$-$SiO_2$@$Fe_3O_4$ Magnetic Nanospheres

$SiO_2$@$Fe_3O_4$ (1.00 g) was dispersed in toluene (100 mL). Then APTES (Silane coupling agent) (10 mL) was added. APTES will bond to the surface of $Fe_3O_4$ nanoparticles to form the ammoniated $NH_2$-$SiO_2$@$Fe_3O_4$. The reaction mixture refluxed at 110 °C for 8 h, and magnetically separated after natural

 doi:10.20944/preprints202402.0937.v1



cooling and washed with toluene and ethanol for four times. Finally, the resultant $NH_2$-$SiO_2$@$Fe_3O_4$ nanocomposites were dried at 60 °C for further use.

Synthesis of COF-$SiO_2$@$Fe_3O_4$ Magnetic Nanoparticles

$NH_2$-$SiO_2$@$Fe_3O_4$ (0.2 g), benzidine (0.185 g) and 3,3,5,5-tetraaldehyde biphenyl (0.133 g) were added into 80 mL DMSO and ultrasonically dispersed for 10 min to form a stable dispersion. Then, add 2.5 mL glacial acetic acid slowly. The mixture was transferred to autoclave, and then heated to 200 °C for 3 days. After reaction, the product was collected by magnet and washed with THF and methanol for several times and then dried at 60 °C in vacuum.

*3.5. MSPE pretreatment*

The prepared COF-$SiO_2$@$Fe_3O_4$ nanocomposites were used to extract PYRs from aqueous sample solution. Firstly, 20 g crushed cabbage sample was put into a centrifuge tube, 20 mL acetonitrile was added, shaken for 20 min, centrifuged at 4500 r·min$^{-1}$ for 15 min, and the supernatant was extracted. The supernatant was evaporated to about 3 mL, blown to nearly dry with nitrogen, and redissolved with ultrapure water to 100 mL. Then 10 mg COF-$SiO_2$@$Fe_3O_4$ nanocomposites were dispersed in 20 mL sample solution under vigorous oscillation for 10 min to adsorb the target analytes until adsorption equilibrium. Then, the COF-$SiO_2$@$Fe_3O_4$ nanocomposites with adsorbed PYRs were collected by using an external magnet and eluted with 1 mL acetone under 3 min of ultrasound. The desorption solution was collected, filtered through a 0.22 μm filter and injected for GC-MS analysis.

*3.6. GC-MS conditions*

The GC was fitted with an Rxi-5si1MS column (30 m × 0.25 mm × 0.25 μm) (Shimadzu, Japan). Helium (99.999% purity) was utilized as the carrier gas. The inlet temperature was 250°C and the sample was injected at 1 μL without splitting (1.08 mL·min$^{-1}$). The initial oven temperature is controlled at 150°C (hold for 0.5 min), then with a rate of 25°C·min$^{-1}$ to 180°C, and finally with a rate of 10°C·min$^{-1}$ to 250°C (hold for 8 min). The ion source temperature, and Interface temperature were 230°C, and 250°C, respectively. The solvent delay was set to 2 min (bypassing the solvent peak). Separation of the PYRs was sufficient to set up the full scan in the range 40–500 m/z. The selected ion monitoring (SIM) mode was used. Sample analysis was performed with the electron ionization source set at 70 eV. The mass spectral parameters of 5 PYRs (50 μg·L$^{-1}$) were shown in Table 3.

**Table 3.** Retention time, qualitative and quantitative ions of 5 PYRs.

| Peak number | Compound | Retention time (min) | Mass-to-charge ratio( m/z) | |
|---|---|---|---|---|
| | | | Quantitative ion | Qualitative ion |
| 1 | Allethrin | 7.440 | 123 | 123, 79, 81 |
| 2 | Tetramethrin 1 | 11.195 | 164 | 164, 123, 81 |
| 3 | Bifenthrin | 11.340 | 181 | 181, 166, 165 |
| 2 | Tetramethrin 2 | 11.440 | 164 | 164, 123, 81 |
| 4 | Fenpropathrin | 11.670 | 97 | 97, 55, 181 |
| 5 | Cyhalothrin | 13.255 | 181 | 181, 197, 208 |

*3.7. Recovery*

Recovery rate (ER) and enrichment factor (EF) were used to evaluate the extraction and enrichment ability of COF-$SiO_2$@$Fe_3O_4$ magnetic nanoparticles on PYRs. The calculation formula are as follows:

$$ER=(C_M \times V_M)/(C_0 \times V_{aq}) \quad (1)$$

$$EF=C_M/C_0 \quad (2)$$

 doi:10.20944/preprints202402.0937.v1



where $C_0$ is the concentration of PYRs added to the sample solution before magnetic solid phase extraction, $C_0$=50 μg·L$^{-1}$. $C_M$ is the concentration of PYRs in acetone elution after magnetic solid phase extraction. $V_{aq}$ represents the volume of sample solution before magnetic solid phase extraction, $V_{aq}$=20 mL. $V_M$ is the volume of acetone eluent after magnetic solid phase extraction.

Experiments were repeated three times to validate the repeatability of the results. The results presented were the average of the three experiments conducted. Origin software was used as statistical treatment to reach the conclusion described in the work.

## 4. Conclusions

In this research, core-shell structured magnetic nanocomposites COF-$SiO_2$@$Fe_3O_4$ were synthesized and utilized as adsorbents for the preconcentration of five PYRs via MSPE. The interaction between the benzene in COF-$SiO_2$@$Fe_3O_4$ and the benzene of analytes facilitated the effective extraction of PYRs from sample solutions. The combination of COF-$SiO_2$@$Fe_3O_4$ based MSPE with GC-MS led to the development of a fast, simple, highly efficient, and sensitive method for the determination of trace PYRs, demonstrating a high enrichment factor, wide linear range, low detection limits, and good reproducibility. Furthermore, the successful application in the selective enrichment and determination of trace PYRs in vegetables suggests that the COF-$SiO_2$@$Fe_3O_4$ nanocomposites hold great potential as a novel adsorbent in sample pretreatment.

**Author Contributions:** This work was carried out with collaboration between all authors. L.Y. and A.X. performed the experimental investigation. Y.H. and Z.S. performed the data curation and the analysis. W.L. wrote the first draft of the manuscript. C.X. and Y.Z. performed the review and editing. L.Y. performed the project administration and the funding acquisition.

**Funding:** This work was supported by Science and Technology Research Project of Colleges and Universities in Hebei Province, China (QN2023074).

**Data Availability Statement:** The data were contained within the article.

**Conflicts of Interest:** The authors declare no conflict of interest.

## References

1. Lin, X.; Mou, R.; Cao, Z.; Cao, Z.; Chen, M. Analysis of pyrethroid pesticides in Chinese vegetables and fruits by GC–MS/MS. *Chem. Pap.* **2018**, *72*, 1953-1962.
2. Fang, Y.; Xu,W.; Zhang,W.; Guang, C.; Mu, W. Microbial elimination of pyrethroids: specific strains and involved enzymes. *Appl. Microbiol. Biot.* **2022**, *106*, 6915-6932.
3. Tang, W.; Wang, D.; Wang, J.; Wu, Z.; Li, L.; Huang, M.; Xu, S.; Yan, D. Pyrethroid pesticide residues in the global environment: An overview. *Chemosphere.* **2018**, *191*, 990-1007.
4. Wang, Q.; Chen, L.; Li, Y.; Yang, J.; Yang, R. Magnetic nanocomposite-based TpPa-$NO_2$ covalent organic framework for the extraction of pyrethroid insecticides in water, vegetable, and fruit samples. *Food Anal. Method.* **2022**, *16*, 71-82.
5. Wu, C.; Yang, S; Meng, Y. Investigation of pH-switchability of hydrophobic deep eutectic solvents for the extraction and preconcentration of triazine herbicides in water samples. *Microchem. J.* **2023**, *194*, 109198.
6. Manzanares, N.; Perez, J.; Campana, A.; Gracia, L. Simple methodology for the determination of mycotoxins in pseudocereals, spelt and rice. *Food Control* **2014**, *36*, 94-101.
7. Xie, Y.; Wu, X.; Song, Y.; Sun, Y.; Tong, K.; Yu, X.; Fan, C.; Chen, H. Screening of 258 pesticide residues in silage using modified QuEChERS with liquid-and gas chromatography-quadrupole/orbitrap mass spectrometry. *Agriculture*, **2022**, *12*, 1231.
8. Erarpat, S.; Bodur, S.; Bakırdere, S. Nanoparticles based extraction strategies for accurate and sensitive determination of different pesticides. *Crit. Rev. Anal.Chem.* **2022**, *52*, 1370-1385.
9. Lin, X.; Wang, X.; Wang, J.; Yuan, Y.; Di, S.; Wang, Z.; Xu, H.; Zhao. H.; Zhao, C.; Ding, W.; Qi, P. Magnetic covalent organic framework as a solid-phase extraction absorbent for sensitive determination of trace organophosphorus pesticides in fatty milk. *J. Chromatogr. A.* **2020**, *1627*, 461387.
10. Hamidi S. Recent advances in solid-phase extraction as a platform for sample preparation in biomarker assay. *Crit. Rev. Anal.Chem.* **2023**, *53*, 199-210.
11. Fu, Q.; Li, J.; Wang, X.; Sun-Waterhouse, D.; Sun, X.; Waterhouse, G.; Wu, P. Covalent organic framework-based magnetic solid-phase extraction coupled with gas chromatography-tandem mass spectrometry for the determination of trace phthalate esters in liquid foods. *Microchim. Acta* **2023**, *190*, 1-11.

 doi:10.20944/preprints202402.0937.v1




12. Wu, G.; Zhang, C.; Liu, C.; Li, X.; Cai, Y.; Wang, M.; Chu, D.; Liu, L.; Meng, T.; Chen, Z. Magnetic tubular nickel@silica-graphene nanocomposites with high preconcentration capacity for organothiophosphate pesticide removal in environmental water: Fabrication, magnetic solid-phase extraction, and trace detection. *J. Hazard. Mater.* **2023**, *457*, 131788.
13. Nasiri, M.; Ahmadzadeh, H.; Amiri, A. Organophosphorus pesticides extraction with polyvinyl alcohol coated magnetic graphene oxide particles and analysis by gas chromatography-mass spectrometry: Application to apple juice and environmental water. *Talanta* **2021**, *227*, 122078.
14. Wei, D.; Pan, A.; Zhang, C.; Guo, M.; Lou, C.; Zhang, J.; Wu, H.; Wang, X. Fast extraction of aflatoxins, ochratoxins and enniatins from maize with magnetic covalent organic framework prior to HPLC-MS/MS detection. *Food Chem.* **2023**, *404*, 134464.
15. Zhao, Y.; Bai, X.; Liu, Y.; Liao, X. Determination of fipronil and its metabolites in egg samples by UHPLC coupled with Q-Exactive high resolution mass spectrometry after magnetic solid-phase extraction. *Microchem. J.* **2021**, *169*, 106540.
16. Liang, S.; Shi, F.; Zhao, Y.;Wang, W. Determination of local anesthetic drugs in human plasma using magnetic solid-phase extraction coupled with high-performance liquid chromatography. *Molecules* **2022**, *27*, 5509.
17. Cui, S.; Mao, X.; Zhang, H.;Zeng, H.; Lin, Z.; Zhang, X.; Qi, P. Magnetic solid-phase extraction based on magnetic sulfonated reduced graphene oxide for HPLC–MS/MS analysis of illegal basic dyes in foods. *Molecules* **2021**, *26*, 7427.
18. Jiang, H.;Yang, S.; Miao, H; Tian,H.; Sun, B. Ultrasonic synthesis of magnetic covalent organic frameworks and application magnetic solid phase extraction for rapid adsorption of trace bisphenols in food samples. *Food Chem.* **2024**, *440*, 138264.
19. Asl, A.; Rafati, A.; Khazalpour, S. Highly sensitive molecularly imprinted polymer-based electrochemical sensor for voltammetric determination of Adenine and Guanine in real samples using gold screen-printed electrode. *J. Mol. Liq.* **2023**, *369*, 120942.
20. Huang, Y.; Li, Y.; Luo, Q.; Huang, X. One-pot strategy as a green and rapid method to fabricate magnetic molecularly imprinted nanoparticles for selective capture of sulfonylurea herbicides. *ACS. Appl. Mater. Interfaces*. **2021**, *13*, 37280-37288.
21. Elancheziyan, M.; Prakasham, K.; Eswaran, M.; Duraisamy, M.; Ganesan, S.; Lee, S.; Ponnusamy, V. Eco-friendly fabrication of nonenzymatic electrochemical sensor based on cobalt/polymelamine/nitrogen-doped graphitic-porous carbon nanohybrid material for glucose monitoring in human blood. *Environ. Res.* **2023**, *223*, 115403.
22. Li, P.; Huang, D.; Huang, J.; Tang, J.; Zhang, P.; Meng, F. Development of magnetic porous carbon nano-fibers for application as adsorbents in the enrichment of trace Sudan dyes in foodstuffs. *J.Chromatogr. A* **2020**, *1625*, 461305.
23. Yu, H.; Bi, X.; He, Y.; Cui, Y.; Yang, C. Microporous organic network: superhydrophobic coating to protect metal–organic frameworks from hydrolytic degradation. *ACS. Appl. Mater. Interfaces* **2023**, *15*, 36822-36830.
24. Li, Z.; Hu, C.; Hu, Z.; Fu, Y.; Chen, Z. Facile synthesis of novel multifunctional β-cyclodextrin microporous organic network and application in efficient removal of bisphenol A from water. *Carbohyd. Polym.* **2022**, *276*, 118786.
25. Abdelhai Senosy, I.; Guo, H.; OuYang, M.; Lu, Z.; Yang, Z.; Li, J. Magnetic solid-phase extraction based on nano-zeolite imidazolate framework-8-functionalized magnetic graphene oxide for the quantification of residual fungicides in water, honey and fruit juices. *Food Chem.* **2020**, *325*, 126944.
26. Safari, M.; Yamini, Y.; Masoomi, M.; Morsali, A.; Mani-Varnosfaderani, A. Magnetic metal-organic frameworks for the extraction of trace amounts of heavy metal ions prior to their determination by ICP-AES. *Microchim. Acta.* **2017**, *184*, 1555-1564.
27. Wang, J.; Huang, Q.; Guo, W.; Guo, D.; Han, Z.; Nie, D. $Fe_3O_4$@ COF (TAPT–DHTA) nanocomposites as magnetic solid-phase extraction adsorbents for simultaneous determination of 9 mycotoxins in fruits by UHPLC–MS/MS. *Toxins* **2023**, *15*, 117.
28. Zhang, X.; Gao, Y.; Li, J.; Yan, J.; Liu, P.; Fan, X.; Song, W. A novel TAPP-DHTA COF cathodic photoelectrochemical immunosensor based on CRISPR/Cas12a-induced nanozyme catalytic generation of heterojunction. *Electrochim. Acta*. **2023**, *441*, 141771.
29. Gao, R.; Bai, J.; Shen, R.; Hao, L.; Huang, C.; Wang ,L.; Li, X. 2D/2D covalent organic framework/CdS Z-scheme heterojunction for enhanced photocatalytic $H_2$ evolution: Insights into interfacial charge transfer mechanism. *J. Mater. Sci. Technol*. **2023**, *137*, 223-231.
30. Zhang, Y.; Zhang, W.; Gong, H.; Jia, Q.; Zhang, W.; Zhang, Z. Fabrication a sensor based on sulfonate-based COF for humidity sensing. *Mater. Lett.* **2022**, *328*, 133123.
31. Ren, X.; Liao, G.; Li, Z.; Qiao, H.; Zhang, Y.; Yu, X.; Wang, B.; Tan, H.; Shi, L.; Qi, X.; Zhang, H. Two-dimensional MOF and COF nanosheets for next-generation optoelectronic applications. *Coordin. Chem. Rev.* **2021**, *435*, 213781.

 doi:10.20944/preprints202402.0937.v1




32. Zhang, W.; Li, Y.; Xing, Z.; Zhao, M.; Fu, Y.; Wang, S.; Ma, H. Ionic COF composite membranes for selective perfluoroalkyl substances separation. *Macromol. Rapid. Comm.* **2023**, *44*, 2200718.
33. Han, S.; You, W.; Lv, S.; Du, C.; Zhang, X.; Zhang, E.; Zhu, J.; Zhang, Y. Ionic liquid modified COF nanosheet interlayered polyamide membranes for elevated nanofiltration performance. *Desalination* **2023**, *548*, 116300.
34. Lu, J.; Zhou, Y.; Ling, L.X.; Zhou, Y.B. Enhanced activation of PMS by a novel Fenton-like composite $Fe_3O_4$/S-$WO_3$ for rapid chloroxylenol degradation. *Chem. Eng. J.* **2022**, *446*, 137067.
35. Chen, L.; He, Y.; Lei, Z.; Gao, C.; Xie, Q.; Tong, P.; Lin, Z. Preparation of core-shell structured magnetic covalent organic framework nanocomposites for magnetic solid-phase extraction of bisphenols from human serum sample. *Talanta* **2018**, *181*, 296–304.
36. Mojtaba, S.; Mehdi, F.;Seyed, A.; Hajir, K. Tetraethylenepentamine-enriched magnetic graphene oxide as a novel Cr(VI) removal adsorbent. *React. Funct. Polym.* **2022**, *180*, 105410.
37. Wang, Q.; Chen, L.; Cui, X.; Zhang, J.; Wang, Y.; Yang, X. Determination of trace bisphenols in milk based on $Fe_3O_4$@$NH_2$-MIL-88 (Fe)@TpPa magnetic solid-phase extraction coupled with HPLC. *Talanta* **2023**, *256*, 124268.
38. Zhong, X.; Liang, W.; Lu, Z.; Lu, Z.; Hu, B. Highly efficient enrichment mechanism of U (VI) and Eu (III) by covalent organic frameworks with intramolecular hydrogen-bonding from solutions. *Appl. Surf. Sci.* **2020**, *504*, 144403.
39. Deng, H.; Li, X.; Peng, Q.; Wang, X.; Chen, J.; Li, Y. Monodisperse magnetic single-crystal ferrite microspheres. *Angew. Chem. Int. Edit.* **2005**, *44*, 2782-2785.